KSCE Journal of Civil Engineering (2019) 23(2):763-776

DOI 10.1007/s12205-018-0156-x

Surveying and Geo-Spatial Information Engineering

pISSN 1226-7988, eISSN 1976-3808
www.springer.com/12205

Landslide Susceptibility Mapping using Relative Frequency and Predictor Rate along Araniko Highway

Tri Dev Acharya* and Dong Ha Lee**

Received October 8, 2017/Revised July 2, 2018/Accepted August 9, 2018 /Published Online December 17, 2018

Abstract

Roads are important infrastructure that brings economic development in a nation by connecting different places. But, in Nepal, many roads are very vulnerable to landslides due to various reasons. Araniko Highway is one of the most landslide affected major road in Nepal lacking study in past. In this study, landslide susceptibility mapping along Dolalghat - Kodari section in Araniko Highway, Nepal, was done by integrating Relative Frequency (RF) and Predictor Rate (PR). PR was applied to the RF to quantify the prediction ability of the conditioning factors while producing Landslide Susceptibility Index (LSI). First, landslide inventory map of 314 landslides was prepared. Then, the database was divided into 70/30 ratio for the training and validating the model. After analysing thirteen landslide conditioning factors, susceptibility map produced using LSI was categorized into five classes. Finally, overall performance of the resulting map was assessed using the receiver operating characteristic curve technique. The success rate and prediction rate curve showed that the area under the curve for RF was 0.606 and 0.581 respectively. The result of this study showed a successful mapping of landslide susceptibility by integrating RF and PR.

Keywords: *landslide, susceptibility, relative frequency, predictor rate, road, araniko highway, Nepal*

1. Introduction

Roads, which links different places, are the most important infrastructure in many countries. It contributes to economic development by bringing many benefits to the public such as improved access to markets and service centres, improved comfort, speed, and safety; and lower vehicle operating costs. But, a poorly maintained roads can constrain mobility, significantly raise vehicle operating costs, increase accident rates and their associated human and property costs, and aggravate isolation, poverty, poor health, and illiteracy in rural communities (Burningham and Stankevich, 2005). Hence, a proper monitoring and maintaining of road network is a crucial for the development of any nation.

Nepal is a landlocked country located along the Himalayas and bordered to the North by China and India to the rest. Conventionally, roads in Himalayan region of Nepal have been built without sufficient attention given to the environmental aspects. In past decade, the construction of roads in rural Himalayan areas has been rapid from local efforts due to the need of road access and interest of local political leaders (Dahal *et al.*, 2006). Most of the roads are poorly aligned and excavated using the cut-and-throw approach. These inappropriately engineered construction of roads alters the landscape of the earth surface and have significant effect on drainage, slope stability, erosion and sediment supply to drainage (Shrestha, 2010; Petley *et al.*, 2007). Also, much of these roads lie along the river banks which further intensifies the effects.

Landslides are a manifestation of slope instability that effects people, land and livelihood (Glade and Crozier, 2005). These are the main obstacle faced by the Himalayan roads in Nepal due to geologically young mountains and extreme weathers (Dahal *et al.*, 2006; Upreti, 2001). Many of the landslides along roadsides in Nepal are triggered by toe cutting of the slope, saturation of land mass by water or erosion by the river flow along its curve (Sthapit and Tennyson, 1991). Well-known road side landslide events are Krishnabhir landslide (2000) in Pritihivi Highway and Jure landslide (2014) in Araniko Highway. Moreover, recent massive earthquakes in 2015 has left these Himalayas scratched, ruptured and vulnerable to landslide. It is a major potential threat for future landslides in case of another earthquake activity or under extreme weather conditions (Mahmood *et al.*, 2015). Cases of sudden landslide or rockfalls damaging vehicles and loss of lives along highways are very common recently (Khatiwada, 2017; Nagarik News, 2017). Fig. 1 shows an example of the landslide near the Tatopani of Araniko Highway which changes over time. It was active before 2005 and was less affected by the earthquake. But after earthquake, many large landslides occurred in that area. These landslides not only block highways but also may lead to poor condition of roads. Hence, an immense need of

*Researcher, Institute of Industrial Technology, Kangwon National University, Chuncheon 24341, Korea (E-mail: tridevacharya@kangwon.ac.kr)
**Member, Assistant Professor, Dept. of Civil Engineering, Kangwon National University, Chuncheon 24341, Korea (Corresponding Author, E-mail: geodesy@kangwon.ac.kr)

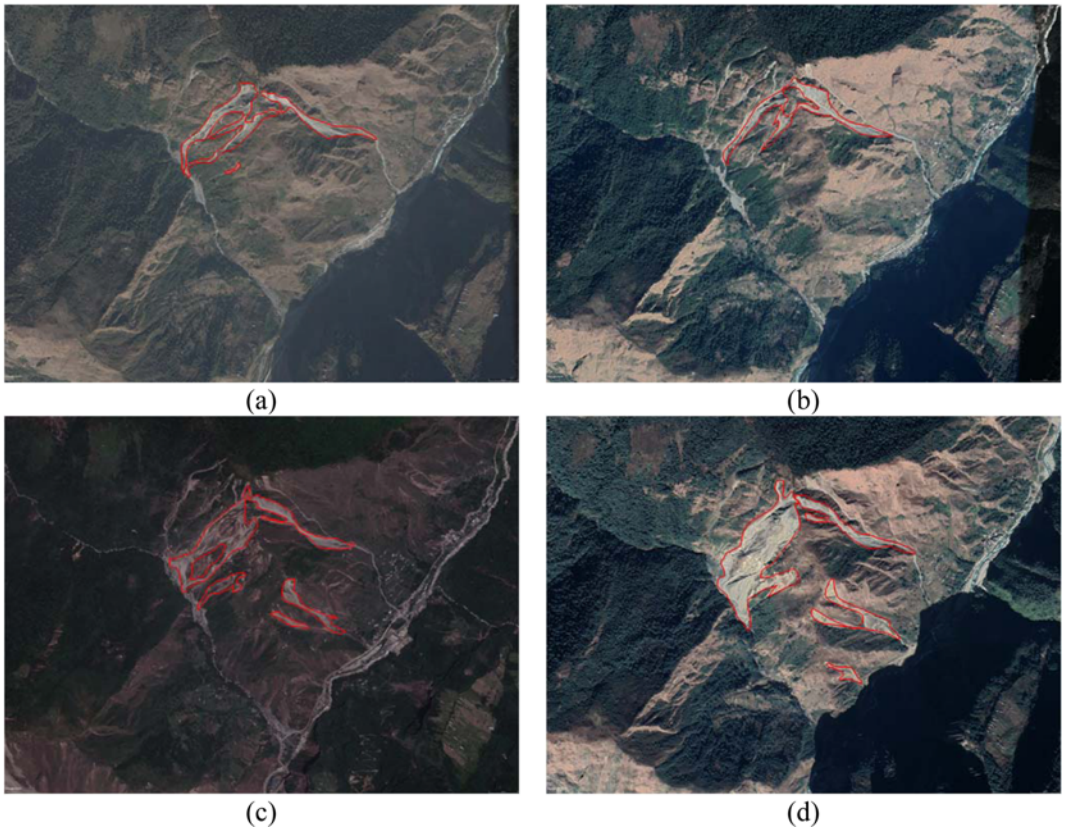

Fig. 1. Change of a Nearby Active Landslide (red polygons) Near Tatopani Section of Araniko Highway. The Images are Taken from Historic Data from Google Earth Pro Dated as: (a) December 06, 2005, (b) December 04, 2014, (c) May 25, 2015, (d) December 09, 2017

understanding spatial distribution of landslides along the highway areas in Nepal.

Landslide susceptibility maps shows areas with high and low landslide prone areas and can be used to take preventive measures in advance before the damage is done (Tien Bui *et al.*, 2014a). Globally, various studies on road section has been carried out in order to map landslide susceptibility and understand the probability of slope failures along them (Hong *et al.*, 2018; Youssef *et al.*, 2015; Regmi *et al.*, 2014a; Tien Bui *et al.*, 2014b; Regmi, *et al.*, 2014b; Timilsina *et al.*, 2014; Devkota *et al.*, 2013; Das *et al.*, 2010; Sidle *et al.*, 2010; Salcedo, 2009). In Nepal also, researchers have done studies in some road section. Devkota *et al.* (2013) applied certainty factor, index of entropy and logistic regression models in GIS and compared the landslide susceptibility results at Mugling–Narayanghat road section in Nepal Himalaya using 321 landslides and 12 conditioning factors. Timilsina *et al.* (2014) derived the landslide distribution probability using logistic regression method in three highways: the Tribhuwan Highway, the Prithivi Highway, and the Narayanghat–Mugling Road using a total of 1489 large-scale landslides with 7 conditioning factors. For rest of the many unexplored places, lack of historical landslide inventory and latest geospatial data are also a very big

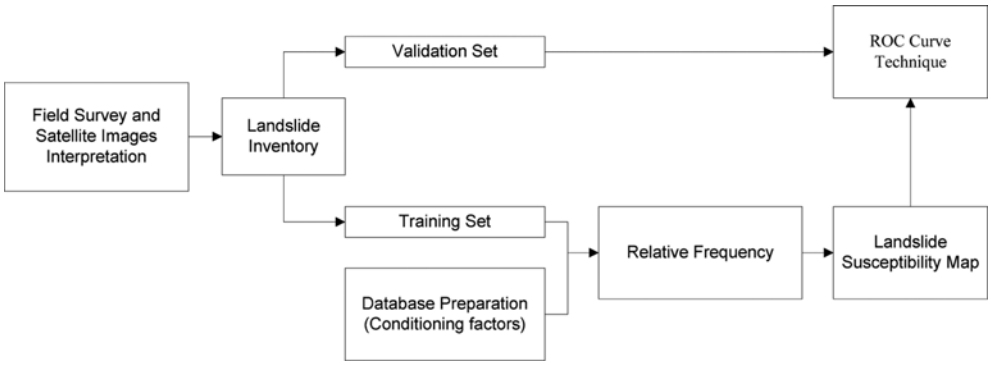

Fig. 2. Flowchart adopted in This Study

issue. Previous study on the area covering Araniko Highway was focused on mostly in regional scale with no focused study on highway (Acharya, 2018; Acharya and Yang, 2015).

In this study, we present first comprehensive landslide susceptibility mapping using Relative Frequency (RF) and Predictor Rate (PR) along Dolalghat - Kodari road section in the Araniko Highway, Nepal. The site is a hilly road that has experienced various landslides activities in past years. However, studies have never been carried out for this area focusing on highway, therefore assessing slope conditions and delineating areas with high probabilities of landslides were vital tasks. We collected as much information regarding the past and current landslide events to develop the landslide inventory along with all the possible conditioning factors. The workflow adopted in the study is shown in Fig. 2. The database and results could be used by planners and decision makers to develop strategies for monitoring of landslide hazard and conduct maintenance and mitigation measures along the road section.

2. Study Area

A road section in Araniko Highway, which provides Nepal's overland link with Tibet and China, is selected for the study area. The section is around 58 kms. in length and starts from Dolaghat (27°38'23.48"N, 85°42'25.87"E), a town at the confluence of the Indravati and the Sun Koshi rivers, along Barabise, a town at confluence of the Bhote Koshi and Sun Koshi rivers confluence of the Bhote Koshi and Sun Koshi rivers ends to Sino-Nepal Friendship Bridge (Nepal-China border), Kodari (27°58'24.45"N, 85°57'49.49"E). The highway section ascends from 630 m to 1736 m and has narrow two lanes blacktopped, gravel roads with bridges. The study area covers about 58 sq. kms. which was selected based on the lineaments within 2 to 3 kms. buffer zone (Fig. 3).

Due to extremely steep slopes on both side of the road, it is one of the most dangerous highways in Nepal particularly past Barabise. The roads sections run along the river sides in extreme steep Himalayan mountains, massive landslides and bus plunges are not uncommon especially after during and after rainfall events. Hence, these sections are likely to be closed temporarily in monsoon seasons i.e. between May and August. A major landslide in 2014 created a large lake that blocked the highway in Jure village area for more than a month, and repairs were still underway when the 2015 earthquake brought more devastation along the road. Beside its economic link of import to China boarder, it is also a very important social link to the people of Sindhupalchowk district. As the road is major network to supply goods and commute, its obstacle can even completely cut of people from one side to another.

Geologically the study area has 9 geological formations which

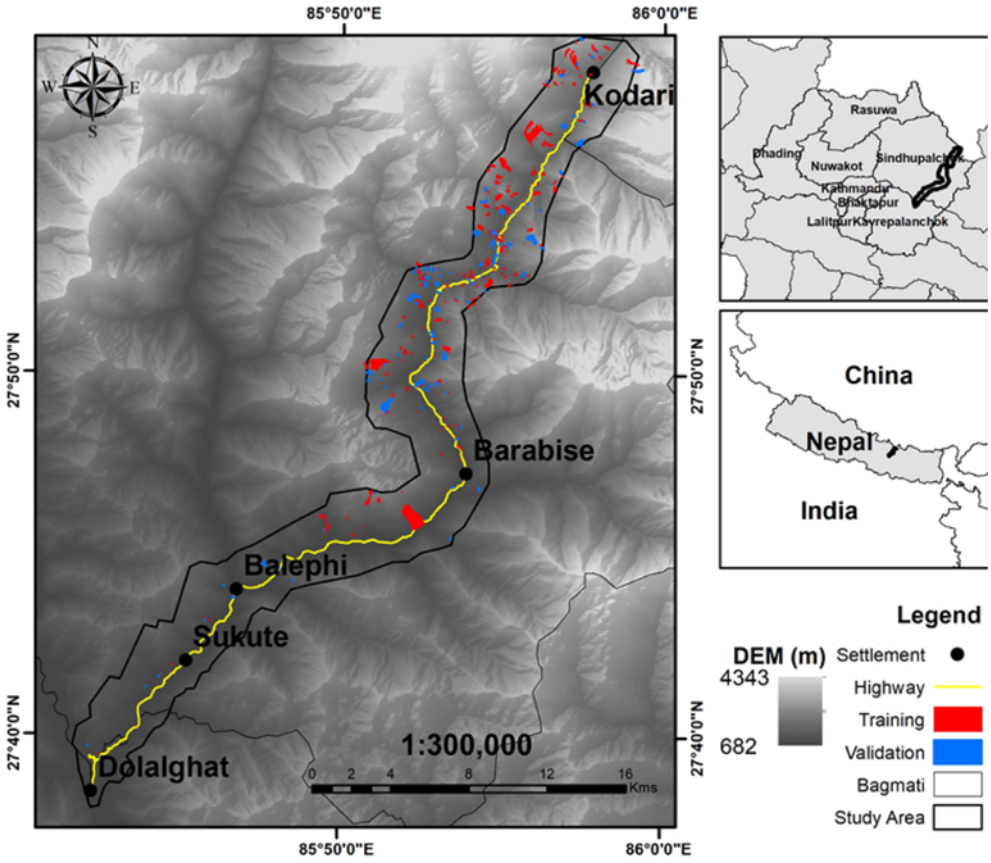

Fig. 3. Location Map of the Study Area and Landslides (training and validation set) in Araniko Highway with Elevation and Major Settlements

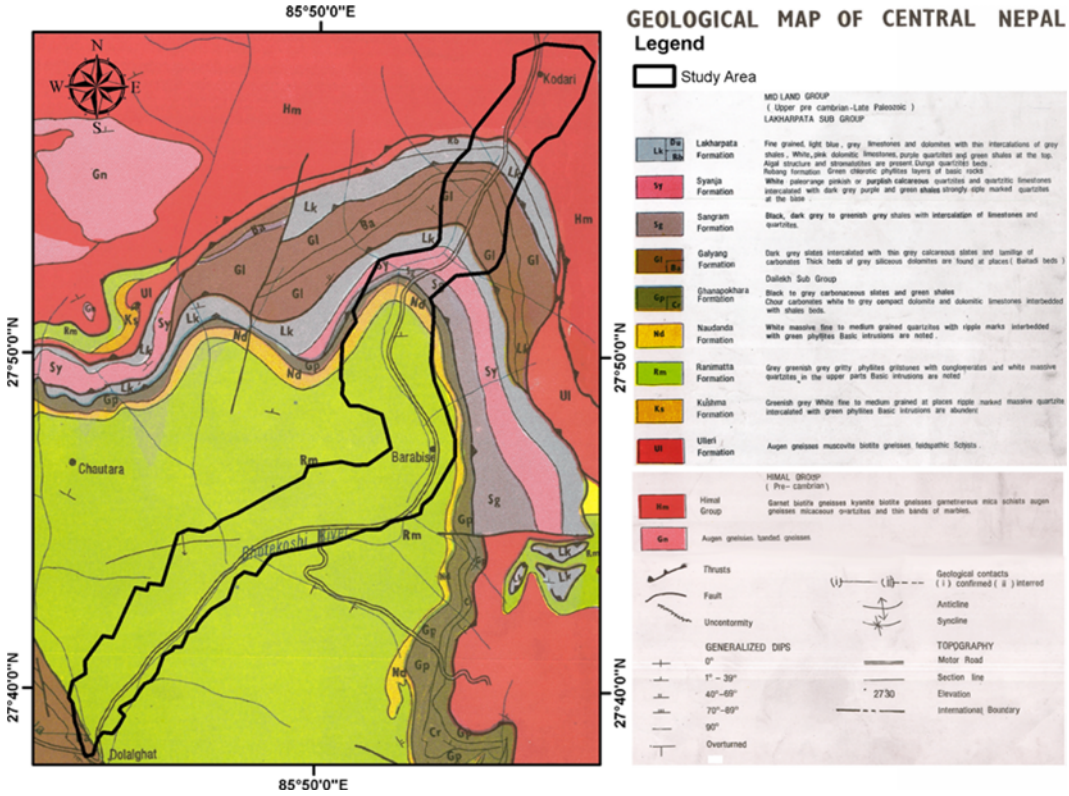

Fig. 4. Geological Map of the Study Area and Its Surroundings (Clipped from Scan of Original Map)

falls in Pre-Cambrian Himal group and upper Pre-cambrian-Late Paleozoic Lakhapatra sub group of Mid Land group (Fig. 4). The study is mostly covered by forest which has been extensively used for agriculture. Settlements along the road sides are aggravated in some major intersections of road whereas rest are sparse rural settlements in hilly slopes.

3. Landslide Inventory and Database Preparation

A landslide susceptibility analysis consists four major steps: collection and construction of spatial database of landslide and conditioning factors, assessment of landslide susceptibility using the relationship between landslide and conditioning factors and last the validation of the results (Guzzetti *et al.*, 1999). And all these available approaches for landslide susceptibility mapping are based upon assumptions that landslides are most likely to occur under similar geomorphological, geological, and hydrogeological and climatic conditions, which were and are responsible for the occurrence of past and present landslides (Yang *et al.*, 2016; Kanungo *et al.*, 2009). Hence, landslide inventory is used to derive the quantitative relationships between the landslide occurrences and conditioning factors.

In this study, the landslide inventory was prepared by two methods, first interpretation of satellite imageries: mid resolution Landsat 8 images and high-resolution images available in Google Earth Pro and field verification (Acharya *et al.*, 2016a). Google Earth is an excellent database of historical high-resolution imageries which can reveal many landslides and landuse changes in the past. Literatures have shown that Google Earth images can be a reliable source for landslide inventory preparation and thus susceptibility mapping in remote areas (Conoscenti *et al.*, 2016; Costanzo *et al.*, 2014; Costanzo *et al.*, 2012). Most of the polygons digitized in the Google Earth were later verified by the field verification (Fig. 5). Removal of false identified or addition of new or undetected were done while in the field work. Extensive field work was carried out after the massive earthquake in 2016 whereas field works for the roadsides were done again in early 2017 for the addition of new landslides. A total of 314 landslides were identified under the study area. In the landslide inventory map, landslide pixels were assigned 1 whereas a "0" were assigned for pixels out of the landslide polygons i.e. non-landslide pixels. In order to evaluate the prediction capability, unused field verified data is a must. Hence, the total landslides events were split into two sets of 70% and 30% randomly, where 221 were used for training remaining 93 for validating the result.

In countries like Nepal, availability of the update to date geospatial data is a very challenging for the researchers. And construction of such database is discouraged by the limited budget and default in reaching remote areas. Hence for this study, we have tried out best in collecting all the data available. A total of thirteen conditioning factors were collected from various sources and used in the study. And all processing was carried out in ArcGIS version 10.3 software package.

A Digital Elevation Model (DEM) is a 3D representation of the

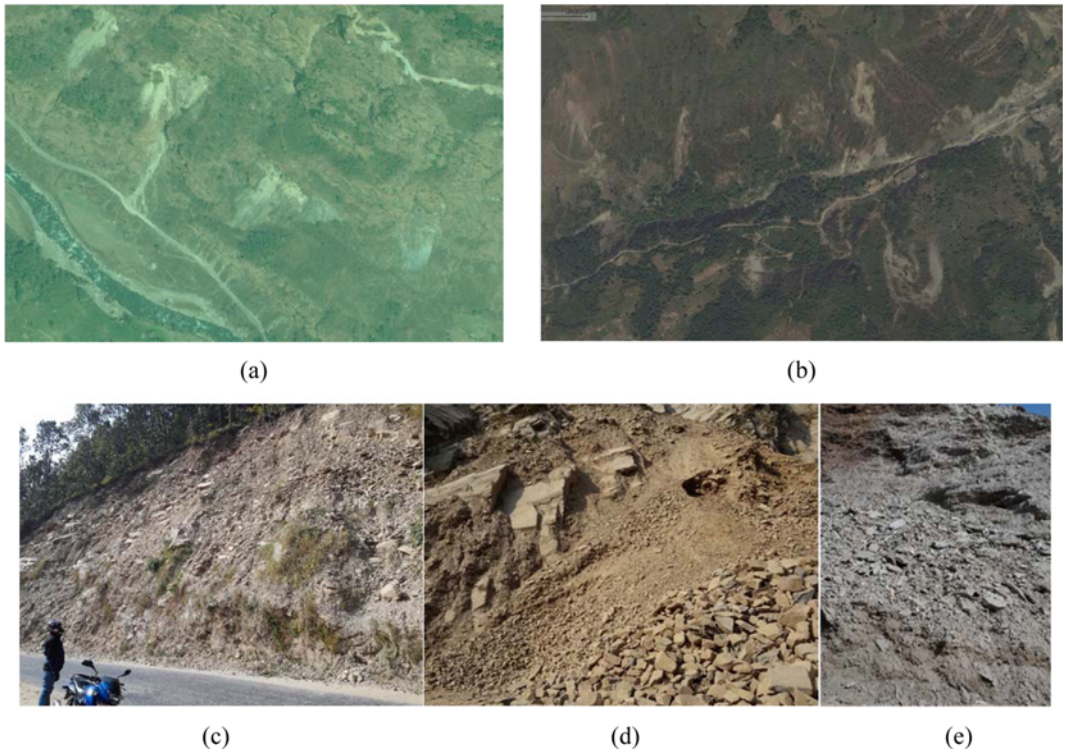

Fig. 5. Preparation of Landslide Inventory Map of the Study Area using: (a, b) Google Earth Pro Satellite Imageries; (c, d, e) Field Verification

terrain and is very useful in preparing many geomorphological derivatives for landslide susceptibility mapping. Digital contour map of 100 m interval and hydro lines of stream extracted from national topographic maps were used for the derivation of 25 × 25 m resolution DEM (Fig. 3). The topographic map was prepared jointly by Department of Survey, Government of Nepal and Japan International Cooperation Agency in 1993 using aerial photographs taken on December 1990 and field verified on December 1991. Using the DEM, six conditioning factors: relief, slope, aspect, curvature, Topographic Wetness Index (TWI), Stream Power Index (SPI) were generated (Figs. 5(a)–5(f)). All these conditioning factors has been used and found to be very important in determining the landslides susceptibility in various studies (Hong *et al.*, 2018; Chen *et al.*, 2017; Pham *et al.*, 2017; Yang *et al.*, 2016; Tien Bui, *et al.*, 2014a; Althuwaynee *et al.*, 2014a; Regmi *et al.*, 2014c).

A 1:250000 scale geological map of central Nepal published by Department of Mines and Geology, Government of Nepal was used to derive the geology of the study area. The printed map was scanned in high resolution and digitized to form the geological map for the study (Fig. 4). Soil map was clipped form the digital dominant soil layer from Soil and Terrain database (SOTER) for Nepal. It is a generalisation of Nepal's Soil and Terrain database at a scale of 1:50 000 compiled in 2004 by FAO and the Survey Department of Nepal together.

As rural areas in Nepal has very sparse settlement and only four major landuse classes are prevalent i.e., water, barren, forest and cultivation, Landsat 8 image taken on November 18, 2013 was used for the derivation of landuse class based on unsupervised ISO clustering method and the 4 classes were categorized based on the high-resolution image of Google Earth. And to match the vegetation in these classes, the same image is also used to derive the Normalized Difference Vegetation Index (NDVI). The bare lands with no vegetation are more prone to landslides than forest or grassland with higher NDVI. Also, NDVI aids in neglecting water bodies where landslides are null.

The river network in any catchment is an outcome of long time interaction between the geological structures, topography and slope under influence of water whereas roads are manmade artificial cuts and fills causing instability of the slope (Tien Bui *et al.*, 2011). Taking account of their conditioning of slope instability, distance to roads and rivers were derived based on Euclidean distance.

Rainfall is one of the main natural triggering factors for the occurrence of landslides. Nepal lies in sub-tropical zone with abundant rainfall in the period of the summer monsoon (June to early October), which, however, penetrates with difficulty in some sheltered inland valleys and on the northern slopes. On the southern slopes, at equal altitude the east is rainier than the west. The annual average rainfall map in millimetres (mm) was retrieved from the Humanitarian Data Exchange (USAID Nepal, 2015), which was created in 2003 using observed data from about 200 stations over a 20-year period (1980–2000).

4. Landslide Susceptibility Mapping and Validation

The susceptibility of landslide in any region can be estimated based on the contribution of causative factors and the relationship

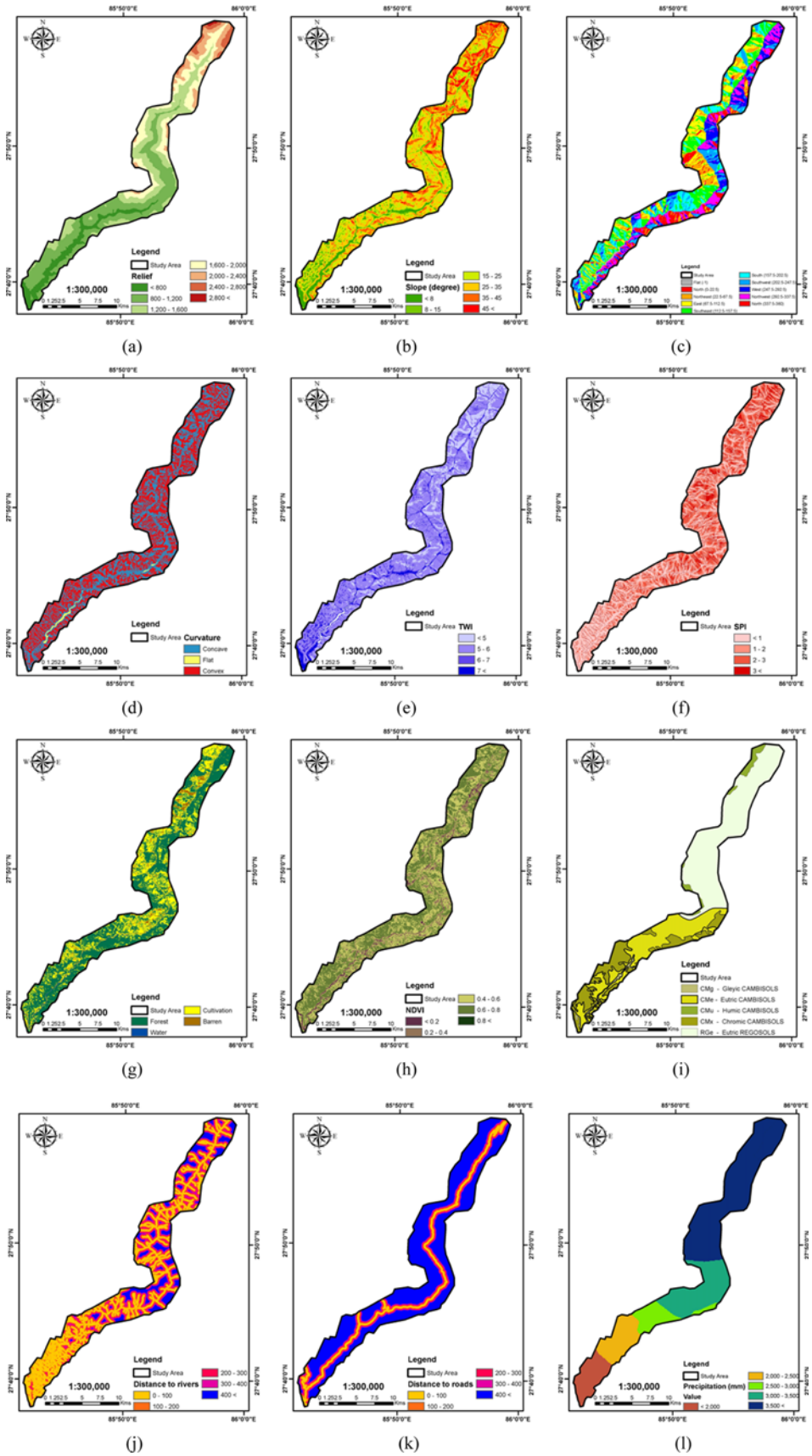

Fig. 6. Thematic Maps of the Study Area: (a) Relief, (b) Slope, (c) Aspect, (d) Curvature, (e) TWI, (f) SPI, (g) Landuse, (h) NDVI, (i) Dominant Soil, (j) Distance to Rivers, (k) Distance to Roads, (l) Annual Average Rainfall

between them. In recent days, machine learning methods are used widely in landslide studies. But these methods require huge data amount as training for better accuracy. Due to the limited data, we used the probabilistic models based on frequency and ratio of landslides in different factors.

Frequency Ratio (FR) is one of the widely used probabilistic model in landslide susceptibility studies due to its simplicity (Yang *et al.*, 2016; Kayastha, 2015; Regmi *et al.*, 2014a; Choi *et al.*, 2012; Yilmaz, 2009; Lee and Sambath, 2006). FR is defined as the ratio of the area where landslides occurred in the total study area and is also the ratio of the probabilities of a landslide occurrence to a non-occurrence for a given attribute (Bonham-Carter, 1994; Lee and Sambath, 2006; Pradhan and Lee, 2010). It is based on the observed relationship between the spatial distribution and causative factors of landslides and can be expressed mathematically as:

$$FR = \frac{N_{pix}(LX_i) \Big/ \sum_{i=1}^{m} N_{pix}(LX_i)}{N_{pix}(X_j) \Big/ \sum_{j=1}^{n} N_{pix}(X_j)} \quad (1)$$

where, FR is the frequency ratio of class *i* of parameter *j*. $N_{pix}(LX_i)$ is the number of pixels with landslides within class *i* of parameter variable *X*. $N_{pix}(X_j)$ is the number of pixels within parameter variable X_j. *m* is the number of classes in the parameter variable X_i, and *n* is the number of parameters in the study area (Regmi *et al.*, 2014c).

As a next step, FRs were normalized in the range of probability values [0,1] as Relative Frequency (RF). The RF for each class were calculated using the following Eq. (2):

$$RF = \frac{FR_{ij}}{\sum_{i=1}^{m} FR_{ij}} \quad (2)$$

After the normalization, the RF frequency has still the drawback of considering all conditioning factors as equal weight. For the purpose to solve the drawback, and to consider the mutual interrelationship among the independent variables, Prediction Rate (PR) was calculated for the rating of every conditioning factor with the training dataset as:

$$PR = \frac{(RF_{\max} - RF_{\min})}{(RF_{\max} - RF_{\min})_{\min}} \quad (3)$$

Finally, the Landslide Susceptibility Index (LSI) was calculated by the summation of product of each factor's PR and each class's RF as shown below:

$$LSI = \sum (PR * RF) \quad (4)$$

Based on these LSI values, a landslide susceptibility map was generated. It is very important that the developed map is accurate and reliable. It should be noted that the LSI used only training dataset and there is remaining 30% for validation.

In order to assess the performance and accuracy of a landslide susceptibility model, widely used Receiver Operating Characteristic (ROC) curve method has been used for this study (Chen *et al.*, 2017; Tien Bui *et al.*, 2016; Althuwaynee *et al.*, 2014b; Pourghasemi *et al.*, 2012). It is a sensitivity or specificity curve that reflects the dynamic changes in classification results. ROC curve is evaluated based on the Area Under the Curve (AUC), i.e., the area between the horizontal axis and the ROC curve (Zhang *et al.*, 2016). The AUC value ranges between 0.5 and 1 and a value more than 0.5 means the model is acceptable (Swets, 1988). The higher the percentage of the area below the curve, i.e. the steeper the curve's slope, the better is the prediction. A value of 0.9 for the AUC would indicate a very good model, in which 90% of the landslides falls in the 10% highest susceptibility area (Lee and Talib, 2005).

5. Result and Discussion

After preparing all the conditioning factors, based on the 70% training dataset, FR and PR of all the class were calculated. Table 1 shows the percentage of landslides and domains, FR, RF as well as PR for each class and factors. In many landslide susceptibility studies, FR is widely used. But, here we have normalized in between 0-1 for better comparison and understanding the influence in calculation of LSI. Also, the PR provides the weightage of the factors influencing the LSI.

In relief factor, range from 1600 to 2800 m shows high value of RF indicating that landslide have occurred more there in past and have probability of landslide in such range. Similarly, Slope above 35° have higher value but above 45° has much higher compared to rest class. Higher relief and higher slope angle are very common causing factors of landslides and has been found in most case studies around the world (Hong *et al.*, 2007). Aspect classes have very widely distributed landslide events. As the road ascends from South to North and most human settlement and farming practices are in southern faced direction, Southern region showed nearly more than 50% of the landslide distribution. The same result was found in previous study by Dahal *et al.* (2008) for lesser Himalaya of Nepal. In contrast, flat surface has also shown landslide distribution in the study which are due to the landslide toe or accumulated zones. The same reason is for the higher distribution of landslide in the flat curvature. Also, concave slopes showed higher landslide occurrence than the concave ones. It is since the convex slopes are more stable as runoffs are dispersed equally whereas concave force water to concentrate at the lower ends (Stocking, 1972).

TWI is the relationship between water accumulation in any location and the gravitational force inclination in the stream that accumulates down the slope (Beven and Kirkby, 1979). In our case also, the TWI has shown the inverse relationship with the landslide susceptibility with higher distribution of landslides having TWI less than 5. SPI has also shown that more the erosion power in a location, the higher chances of slope failure with gradual increase in landslide distribution with SPI value.

In case of landuse, the barren surface showed much higher RF which are also in fact the areas with lowest NDVI. In addition, these areas are highly erodible thus have higher SPI also. Forest areas showed lesser landslide occurrence compared to the

cultivation lands even though both have high NDVI. RF of NDVI shows that it is not necessary that higher NDVI shows better slope stability. One interesting fact is that 7% of the landslides fell in the water area which is due to the difference in the date of images used for the landuse and inventory preparation date. To avoid such confusing findings, some studies have excluded the areas of water bodes for analysis (Zhang *et al.*, 2016).

Now looking to the composition of the study area, Fig. 6(i) shows that most of the area is covered by the Regosols (R) and Cambisols group (C). More than 85% of landslides used for training fall in Cambisol group and among the subgroup about

Table 1. Frequency Ratio (FR), Relative Frequency (RF) and Prediction Rate (PR) of Each Class within Each Factor in the Study Area

Factors	Classes	Landslides pixels (%)	Domain Pixels (%)	FR	RF	$RF_{max} - RF_{min}$	PR
Relief	<800	10.157	2.367	0.233	0.028	0.244	3.277
	800 - 1,200	34.558	18.193	0.526	0.063		
	1,200 - 1,600	24.274	25.035	1.031	0.123		
	1,600 - 2,000	18.055	29.181	1.616	0.193		
	2,000 - 2,400	9.145	17.053	1.865	0.222		
	2,400 - 2,800	3.461	7.878	2.276	0.271		
	2,800 <	0.35	0.294	0.839	0.1		
	Sum	100	100	8.387			
Slope (degree)	< 8	6.679	2.764	0.414	0.05	0.518	6.964
	8 - 15	8.796	2.073	0.236	0.028		
	15 - 25	26.79	6.444	0.241	0.029		
	25 - 35	33.158	23.791	0.718	0.086		
	35 - 45	19.884	43.504	2.188	0.262		
	45 <	4.694	21.424	4.564	0.546		
	Sum	100	100	8.36			
Aspect	Flat	0.784	1.14	1.455	0.158	0.188	2.534
	North	4.325	2.419	0.559	0.061		
	Northeast	10.12	3.576	0.353	0.038		
	East	13.705	6.116	0.446	0.048		
	Southeast	18.309	37.232	2.034	0.22		
	South	12.508	19.61	1.568	0.17		
	Southwest	11.221	15.947	1.421	0.154		
	West	12.122	8.569	0.707	0.077		
	Northwest	12.499	3.697	0.296	0.032		
	North	4.408	1.693	0.384	0.042		
	Sum	100	100	9.224			
Curvature	Concave	43.24	52.073	1.204	0.356	0.151	2.024
	Flat	0.924	1.244	1.346	0.397		
	Convex	55.836	46.683	0.836	0.247		
	Sum	100	100	3.386			
TWI	< 5	20.183	55.01	2.726	0.638	0.56	7.533
	5 - 6	60.748	36.697	0.604	0.141		
	6 - 7	12.07	4.008	0.332	0.078		
	7 <	6.999	4.285	0.612	0.143		
	Sum	100	100	4.274			
SPI	< 1	34.723	15.29	0.44	0.094	0.275	3.694
	1 - 2	29.924	24.862	0.831	0.178		
	2 - 3	23.776	39.893	1.678	0.359		
	3 <	11.577	19.955	1.724	0.369		
	Sum	100	100	4.673			
Landuse	Forest	59.398	31.901	0.537	0.086	0.571	7.674
	Water	1.055	0.449	0.425	0.068		
	Cultivation	33.452	43.341	1.296	0.207		
	Barren	6.095	24.309	3.988	0.639		
	Sum	100	100	6.246			

Table 1. (continued)

Factors	Classes	Landslides pixels (%)	Domain Pixels (%)	FR	RF	$RF_{max} - RF_{min}$	PR
NDVI	< 0.2	2.883	7.153	2.481	0.371	0.25	3.367
	0.2-0.4	9.871	11.468	1.162	0.174		
	0.4-0.6	38.583	42.034	1.089	0.163		
	0.6-0.8	48.497	39.155	0.807	0.121		
	0.8 <	0.166	0.19	1.146	0.171		
	Sum	100	100	6.686			
Soil	CMu	3.803	9.502	2.498	0.282	0.409	5.505
	RGe	50.045	66.586	1.331	0.15		
	CMg	1.682	0	0	0		
	CMx	16.877	23.652	1.401	0.158		
	CMe	27.593	100	3.624	0.409		
	Sum	100	100	8.855			
Distance to Rivers	0-100	41.54	35.048	0.844	0.155	0.105	1.415
	100-200	22.377	23.189	1.036	0.191		
	200-300	13.644	16.641	1.22	0.225		
	300-400	9.207	13.027	1.415	0.261		
	400<	13.232	12.094	0.914	0.168		
	Sum	100	100	5.429			
Distance to Roads	0-100	8.86	6.638	0.749	0.163	0.074	1
	100-200	7.298	5.815	0.797	0.174		
	200-300	6.743	6.05	0.897	0.196		
	300-400	6.817	7.432	1.09	0.238		
	400<	70.282	74.065	1.054	0.23		
	Sum	100	100	4.587			
Precipitation (mm)	<2000	10.618	0.121	0.011	0.004	0.544	7.324
	2000-2500	12.446	0.311	0.025	0.009		
	2500-3000	8.886	0.155	0.017	0.006		
	3000-3500	21.571	26.641	1.235	0.433		
	3500<	46.479	72.771	1.566	0.548		
	Sum	100	100	2.855			
Geology	Sg	1.724	0.916	0.531	0.045	0.259	3.479
	Sy	2.955	5.771	1.953	0.166		
	Lk	4.456	8.103	1.818	0.154		
	Gl	8.7	17.433	2.004	0.17		
	Hm	12.843	23.955	1.865	0.158		
	Gp	1.258	0.035	0.027	0.002		
	Nd	3.052	9.295	3.046	0.259		
	Rm	64.654	34.493	0.534	0.045		
	Ba	0.358	0	0	0		
	Sum	100	100	11.778			

40% of the total are in Eutric subgroup. The geology is unique, and formations are concentrated in a small area as we can see in Fig. 4. The FR of the Ratamata formation is very high yet the RF is low. The formations like Lakharpata, Galyang, Syanja and Naudanda have higher RF despite of very few aerial coverages.

River network is very important geomorphological features in any catchment area. In Nepal, most of the roads are made along the river banks due to ease in construction and dumping slope cuts. Even though these slopes near to the rivers and cut roads are prone to slope failures, in case of the Araniko Highway, these are uniformly distributed across the distance. This could be since road and river are located side by side from beginning to the end and landslides are more concentrated around the upper section of the road.

Landslides are naturally triggered by the rainfall and earthquakes. The study collected landslides after the earthquake events but due to the lack of data regarding the landslides, only precipitation data was used. As the road ascents, the annual average rainfall increases and based on the RF, precipitation above 3000 has more relative frequency of landslide occurrence. It can be

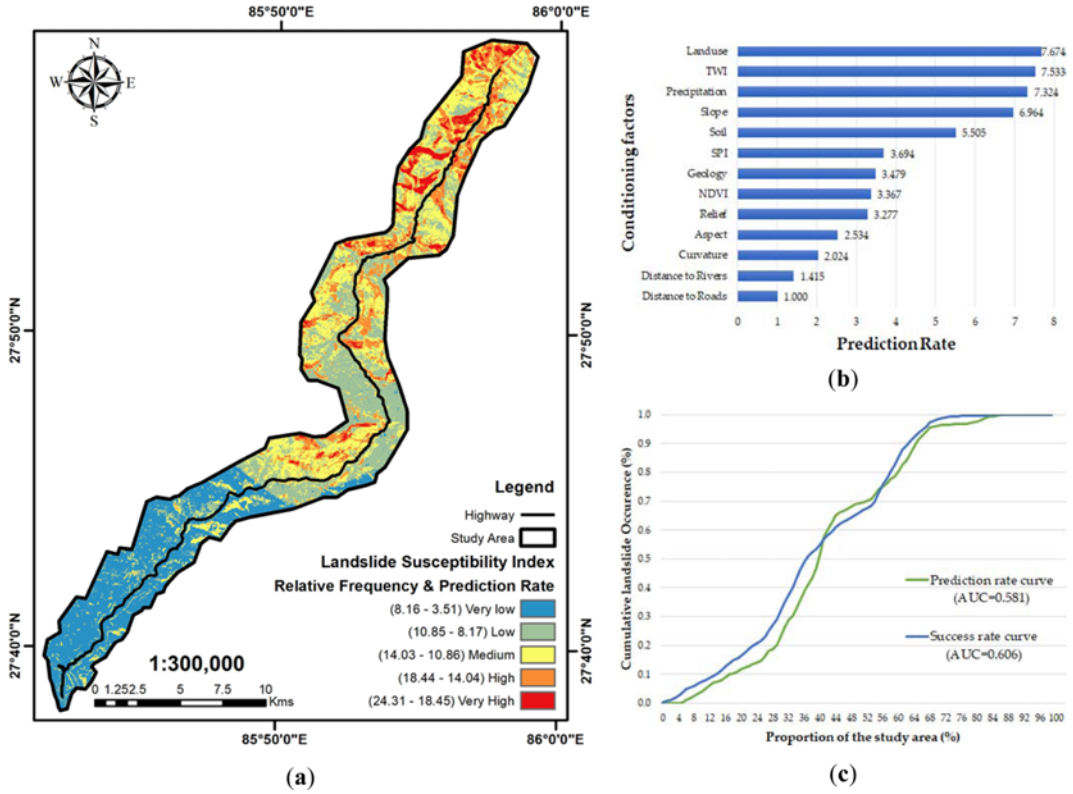

Fig. 7. (a) Landslide Susceptibility Index Map: (b) Prediction Rate of the Conditioning Factors, (c) ROC Curves using Validation and Training Dataset

interpreted as higher rainfall causes higher probability of landslides.

In case of PR, we can see from Table 1 and Fig. 7(a) that landuse, has highest value for PR closely followed by TWI, precipitation and Slope. Soil, geology, NDVI, and relief have medium influence in prediction of landslide occurrence. Distance to roads, distance to rivers, curvature and aspect are the least important conditioning factors in the study.

The LSI value calculated from PR and RF of the thirteen conditioning factors ranged from 3.51 to 24.31 (Table 2). Based on the range of LSI values, the total area was divided into five discrete susceptibility classes: very low, low, medium, high and very high according to the natural break (jenks) method. Fig. 7(a) shows the landslide susceptibility map based on the classification in Table 2. In the study area, around 50% of the area shows very low to low susceptibility along with 25% medium susceptibility of landslide. Only less than 20% of the whole area represents the high and very high susceptibility classes.

Table 2. The Range, Area and Area Percentage of the Five Landslide Susceptibility Classes

Class	Range	Area (sq. km.)	Areal percentage (%)
Very low	3.51 – 8.16	47.28	25.72
Low	8.17 – 14.03	50.49	27.47
Medium	10.86 – 14.03	50.47	27.46
High	14.04 – 18.44	27.93	15.19
Very high	18.45 – 24.31	7.65	4.16

As stated above, ROC curve was applied in this study for the assessment of result. Based on the training dataset, success rate curve was derived and similarly based on the remaining validation dataset prediction rate curve was derived. The ROC curves for both cases are shown in Fig. 7(c). According to the curve, AUC value for training dataset is 0.606 and validation dataset is 0.581. In general, statistical approaches obtain higher AUC value (Chen *et al.*, 2017; Tien Bui *et al.*, 2016; Yang *et al.*, 2016; Althuwaynee *et al.*, 2014b). But, AUC obtained in this study is lower than found in most of the literatures. Although low, the AUC value above 0.5 is acceptable and has been found in many studies with complex study area (Zhang *et al.*, 2016; Bălteanu *et al.*, 2010). The lower value obtained shows either some limitations of the model or improper selection of conditioning factors and sampling training dataset. It could also be due to the longitudinal selection of study area, and a result of complex distribution of the landslides triggered by the 2015 massive earthquakes. For example, the case of northern Pakistan after 2005 Kashmir earthquake (Kamp *et al.*, 2008).

The multiple effect of precipitation and the soil type distribution has segregated the study area in very vivid two categories. As the barren class in landuse, TWI less than 5, and annual average precipitation more than 3500 class in areas with slopes greater than 35° shows lies in the upper section of the study area, the risk at the upper section of the highway is very dangerous. Landslides along the Araniko Highway are long existed and are frequently

Fig. 8. Situation of the Araniko Highway after Earthquake (Sapkota, 2017): (a) Tatopani Bazar, (b) Bhote Koshi River Bank, (c) Phulping Bridge, (d) Damaged Road

erupted into large events such as of Jure landslide in 2014 (Acharya *et al.*, 2016b) and many in past. Fig. 8 shows very poor situation of the road section after the earthquake, which proves the result of the study (Fig. 8). The earthquake triggered landslides destroyed buildings are the edge of the roads along the river and has now been abandoned by the Chinese side for the customs purpose. And, the Tatopani Customs, then only land boarded trade point to China is now abandoned. Moreover, a recent landslide broke Phulping Bridge at Larcha has been destroyed disconnecting the motorable road to Khasa, China through Tatopani, Nepal.

Studies like these should be regularly conducted that are best modelled from the updated inventories. The resulting maps could be easily applicable to the public. The identification risky areas should be evacuated for prevention of further loss of life and property. Based on the landslide susceptibility maps, warning system can also be implemented. Moreover, regional scale adoption of landslide susceptibility maps can also be used for the landslide-safe automatic route planning for a highly rugged hilly terrain (Saha *et al.*, 2005). These measures can be helpful in maintaining sustainable life and economy along the road corridors in hilly regions of Nepal.

6. Conclusions

Roads in hilly regions require very careful monitoring for landslide and related disasters. Nepal faced massive earthquake events in 2015 and left roads vulnerable. In this study, we selected one of the major highway section i.e. Dolalghat – Kodari of Araniko Highway for landslide susceptibility mapping. A complete inventory of landslide was constructed for the study area from field works and image digiting in Google Earth. The Relative Frequency method was used to establish relationship between the conditioning factors and the landslide events in the study area based on the 70% training data, and Prediction Rate was used as weightage for each factor to calculate the Landslide Susceptibility Index.

Based on the LSI, five susceptible classes were derived for the highway corridor and found that only around 20% of the area has high landslide susceptibility. Landslides were distributed mostly in barren lands, slopes higher that 35° at the elevation of 1600 to 2800 meters. Moreover, higher annual precipitation areas have high landslide occurrence but with lesser TWI and lesser NDVI i.e. sloppy hills with shrub and grasslands. This shows, that most of the landslide occurrence are due to the natural factors. The success and prediction rates of the model were satisfactory and acceptable for such complex longitudinal section of road affected by earthquake events. Hence, the result can be a valuable information for the locals for identifying and avoiding the hazardous areas as well as for related authorities for implementing hazard mitigation measures along the highway,

Acknowledgements

This research was supported by Basic Science Research Program

through the National Research Foundation of Korea (NRF) funded by the Ministry of Science, ICT & Future Planning (No.2018R1A2B6009363). The authors are grateful to the Mr. Nab Raj Subedi, Chief Survey Officer, National Landuse Project, Kathmandu and Mr. Sharad Chandra Mainali, Survey Officer, District Survey Office, Chautara at the time of data collection. Also, we would like to thank the anonymous reviewers for their constructive comments and improving this manuscript.

References

Acharya, T. D. (2018). *Regional scale landslide hazard assessment using machine learning methods in Nepal,* PhD Thesis, Kangwon National University, Chuncheon, Korea.

Acharya, T. D., Mainali, S. C., Yang, I. T., and Lee, D. H. (2016a). "Analysis of Jure landslide dam, Sindhupalchowk using GIS and remote sensing." *ISPRS - International Archives of the Photogrammetry, Remote Sensing and Spatial Information Sciences*, Vol. XLI-B6, pp. 201-203, DOI: 10.5194/isprsarchives-xli-b6-201-2016.

Acharya, T. D. and Yang, I. T. (2015). "Landslide hazard zonation using GIS: A case study from Sindhupalchowk, Nepal." *International Journal of Applied Engineering Research (IJAER)*, Vol. 10, No. 7, pp. 18385-18394.

Acharya, T. D., Yang, I. T., and Lee, D. H. (2016b). "Geospatial technologies for landslide inventory: Application and analysis to earthquake-triggered landslide of Sindhupalchowk, Nepal." *Journal of the Korean Society for Geo-spatial Information Science*, Vol. 24, No. 2, pp. 95-106, DOI: 10.7319/kogsis.2016.24.2.095.

Althuwaynee, O. F., Pradhan, B., Park, H. J., and Lee, J. H. (2014a). "A novel ensemble bivariate statistical evidential belief function with knowledge-based analytical hierarchy process and multivariate statistical logistic regression for landslide susceptibility mapping." *Catena*, Vol. 114, pp. 21-36, DOI: 10.1016/j.catena.2013.10.011.

Althuwaynee, O. F., Pradhan, B., Park, H. J., and Lee, J. H. (2014b). "A novel ensemble decision tree-based CHi-squared Automatic Interaction Detection (CHAID) and multivariate logistic regression models in landslide susceptibility mapping." *Landslides*, Vol. 11, No. 6, pp. 1063-1078, DOI: 10.1007/s10346-014-0466-0.

Bălteanu, D., Chendeş, V., Sima, M., and Enciu, P. (2010). "A country-wide spatial assessment of landslide susceptibility in Romania." *Geomorphology*, Vol. 124, No. 3, pp. 102-112, DOI: 10.1016/j.geomorph.2010.03.005.

Beven, K. J. and Kirkby, M. J. (1979). "A physically based, variable contributing area model of basin hydrology / Un modèle à base physique de zone d'appel variable de l'hydrologie du bassin versant." *Hydrological Sciences Bulletin*, Vol. 24, No. 1, pp. 43-69, DOI: 10.1080/02626667909491834.

Bonham-Carter, G. F. (1994). "Geographic information systems for geoscientists-modeling with GIS." *Computer Methods in the Geoscientists*, Vol. 13, pp. 398, DOI: 10.1016/C2013-0-03864-9.

Burningham, S. and Stankevich, N. (2005). "Why road maintenance is important and how to get it done The World Bank, Washington DC Transport Note No." *TRN-4 June, http://hdl.handle.net/10986/11779.*

Chen, W., Xie, X., Wang, J., Pradhan, B., Hong, H., Tien Bui, D., Duan, Z., and Ma, J. (2017). "A comparative study of logistic model tree, random forest, and classification and regression tree models for spatial prediction of landslide susceptibility." *Catena*, Vol. 151, pp. 147-160, DOI: 10.1016/j.catena.2016.11.032.

Choi, J., Oh, H., Lee, H., Lee, C., and Lee, S. (2012). "Combining landslide susceptibility maps obtained from frequency ratio, logistic regression, and artificial neural network models using ASTER images and GIS." *Eng. Geol.*, Vol. 124, pp. 12-23, DOI: 10.1016/j.enggeo.2011.09.011.

Conoscenti, C., Rotigliano, E., Cama, M., Caraballo-Arias, N. A., Lombardo, L., and Agnesi, V. (2016). "Exploring the effect of absence selection on landslide susceptibility models: A case study in Sicily, Italy." *Geomorphology*, No. Supplement C, Vol. 261, pp. 222-235, DOI: 10.1016/j.geomorph.2016.03.006.

Costanzo, D., Cappadonia, C., Conoscenti, C., and Rotigliano, E. (2012). "Exporting a Google Earth™ aided earth-flow susceptibility model: A test in central Sicily." *Nat. Hazards*, Vol. 61, No. 1, pp. 103-114, DOI: 10.1007/s11069-011-9870-0.

Costanzo, D., Chacón, J., Conoscenti, C., Irigaray, C., and Rotigliano, E. (2014). "Forward logistic regression for earth-flow landslide susceptibility assessment in the Platani river basin (southern Sicily, Italy)." *Landslides*, Vol. 11, No. 4, pp. 639-653, DOI: 10.1007/s10346-013-0415-3.

Dahal, R. K., Hasegawa, S., Masuda, T., and Yamanaka, M. (2006). "Roadside slope failures in Nepal during torrential rainfall and their mitigation." *Disaster Mitigation of Debris Flows, Slope Failures and Landslides*, pp. 503-514.

Dahal, R. K., Hasegawa, S., Nonomura, A., Yamanaka, M., Dhakal, S., and Paudyal, P. (2008). "Predictive modelling of rainfall-induced landslide hazard in the Lesser Himalaya of Nepal based on weights-of-evidence." *Geomorphology*, Vol. 102, Nos. 3-4, pp. 496-510, DOI: 10.1016/j.geomorph.2008.05.041.

Das, I., Sahoo, S., van Westen, C., Stein, A., and Hack, R. (2010). "Landslide susceptibility assessment using logistic regression and its comparison with a rock mass classification system, along a road section in the northern Himalayas (India)." *Geomorphology*, Vol. 114, No. 4, pp. 627-637, DOI: 10.1016/j.geomorph.2009.09.023.

Devkota, K., Regmi, A., Pourghasemi, H., Yoshida, K., Pradhan, B., Ryu, I., Dhital, M., and Althuwaynee, O. (2013). "Landslide susceptibility mapping using certainty factor, index of entropy and logistic regression models in GIS and their comparison at Mugling–Narayanghat road section in Nepal Himalaya." *Nat. Hazards*, Vol. 65, No. 1, pp. 135-165, DOI: 10.1007/s11069-012-0347-6.

Glade, T. and Crozier, M. J. (2005). "The nature of landslide hazard impact." *Landslide Hazard and Risk*, T. Glade, M. Anderson, and M. Crozier, Ed., John Wiley & Sons, Ltd., Chichester, West Sussex, England, pp. 43-74, DOI: 10.1002/9780470012659.ch2.

Guzzetti, F., Carrara, A., Cardinali, M., and Reichenbach, P. (1999). "Landslide hazard evaluation: A review of current techniques and their application in a multi-scale study, Central Italy." *Geomorphology*, Vol. 31, Nos. 1-4, pp. 181-216, DOI: 10.1016/s0169-555x(99)00078-1.

Hong, Y., Adler, R., and Huffman, G. (2007). "Use of satellite remote sensing data in the mapping of global landslide susceptibility." *Nat. Hazards*, Vol. 43, No. 2, pp. 245-256, DOI: 10.1007/s11069-006-9104-z.

Hong, H., Liu, J., Bui, D. T., Pradhan, B., Acharya, T. D., Pham, B. T., Zhu, A., Chen, W., and Ahmad, B. B. (2018). "Landslide susceptibility mapping using J48 Decision Tree with AdaBoost, Bagging and Rotation Forest ensembles in the Guangchang area (China)." *Catena*, Vol. 163, pp. 399-413, DOI: 10.1016/j.catena.2018.01.005.

Kamp, U., Growley, B. J., Khattak, G. A., and Owen, L. A. (2008). "GIS-based landslide susceptibility mapping for the 2005 Kashmir earthquake region." *Geomorphology*, Vol. 101, No. 4, pp. 631-642, DOI: 10.1016/j.geomorph.2008.03.003.

Kanungo, D., Arora, M., Sarkar, S., and Gupta, R. (2009). "Landslide Susceptibility Zonation (LSZ) Mapping–A Review." *Journal of South Asia Disaster Studies*, Vol. 2, No. 1, pp. 81-105.

Kayastha, P. (2015). "Landslide susceptibility mapping and factor effect analysis using frequency ratio in a catchment scale: A case study from Garuwa sub-basin, East Nepal." *Arabian Journal of Geosciences*, pp. 1-13, DOI: 10.1007/s12517-015-1831-6.

Khatiwada, R. (2017). "This is how landslide has fallen at Narayanghad-Mughlin Road." Vol. 2017, http://ujyaaloonline.com/news/73391.

Lee, S. and Talib, J. A. (2005). "Probabilistic landslide susceptibility and factor effect analysis." *Environ. Geol.*, Vol. 47, No. 7, pp. 982-990, DOI: 10.1007/s00254-005-1228-z.

Lee, S. and Sambath, T. (2006). "Landslide susceptibility mapping in the Damrei Romel area, Cambodia using frequency ratio and logistic regression models." *Environ. Geol.*, Vol. 50, No. 6, pp. 847-855, DOI: 10.1007/s00254-006-0256-7.

Mahmood, I., Qureshi, S. N., Tariq, S., Atique, L., and Iqbal, M. F. (2015). "Analysis of Landslides Triggered by October 2005, Kashmir Earthquake." *PLoS Curr.*, Vol. 7, pp. 1-11, DOI: 10.1371/currents.dis. 0bc3ebc5b8adf5c7fe9fd3d702d44a99.

Nagarik News (2017). "Again landslide in Narayanghad-Muglin Highway." *Traffic Stops*, http://www.nagariknews.com/news/18055.

Petley, D., Hearn, G., Hart, A., Rosser, N., Dunning, S., Oven, K., and Mitchell, W. (2007). "Trends in landslide occurrence in Nepal." *Nat. Hazards*, Vol. 43, No. 1, pp. 23-44, DOI: 10.1007/s11069-006-9100-3.

Pham, B. T., Tien Bui, D., Prakash, I., and Dholakia, M. B. (2017). "Hybrid integration of Multilayer Perceptron Neural Networks and machine learning ensembles for landslide susceptibility assessment at Himalayan area (India) using GIS." *Catena*, Vol. 149, Part 1, pp. 52-63, DOI: 10.1016/j.catena.2016.09.007.

Pourghasemi, H., Pradhan, B., and Gokceoglu, C. (2012). "Application of fuzzy logic and Analytical Hierarchy Process (AHP) to landslide susceptibility mapping at Haraz watershed, Iran." *Nat. Hazards*, Vol. 63, No. 2, pp. 965-996, DOI: 10.1007/s11069-012-0217-2.

Pradhan, B. and Lee, S. (2010). "Landslide susceptibility assessment and factor effect analysis: Backpropagation artificial neural networks and their comparison with frequency ratio and bivariate logistic regression modelling." *Environmental Modelling & Software*, Vol. 25, No. 6, pp. 747-759, DOI: 10.1016/j.envsoft.2009.10.016.

Regmi, A. D., Devkota, K. C., Yoshida, K., Pradhan, B., Pourghasemi, H., Kumamoto, T., and Akgun, A. (2014a). "Application of frequency ratio, statistical index, and weights-of-evidence models and their comparison in landslide susceptibility mapping in Central Nepal Himalaya." *Arabian Journal of Geosciences*, Vol. 7, No. 2, pp. 725-742, DOI: 10.1007/s12517-012-0807-z.

Regmi, A. D., Yoshida, K., Nagata, H., and Pradhan, B. (2014b). "Rock toppling assessment at Mugling–Narayanghat road section: 'A case study from Mauri Khola landslide', Nepal." *Catena*, Vol. 114, pp. 67-77, DOI: 10.1016/j.catena.2013.10.013.

Regmi, A. D., Yoshida, K., Pourghasemi, H. R., Dhital, M. R., and Pradhan, B. (2014c). "Landslide susceptibility mapping along Bhalubang – Shiwapur area of mid-Western Nepal using frequency ratio and conditional probability models." *Journal of Mountain Science*, Vol. 11, No. 5, pp. 1266-1285, DOI: 10.1007/s11629-013-2847-6.

Saha, A. K., Arora, M. K., Gupta, R. P., Virdi, M. L., and Csaplovics, E. (2005). "GIS-based route planning in landslide-prone areas." *Int. J. Geogr. Inf. Sci.*, Vol. 19, No. 10, pp. 1149-1175, DOI: 10.1080/13658810500105887.

Salcedo, D. A. (2009). "Behavior of a landslide prior to inducing a viaduct failure, Caracas–La Guaira highway, Venezuela." *Eng. Geol.*, Vol. 109, Nos. 1-2, pp. 16-30, DOI: 10.1016/j.enggeo.2009.02.001.

Sapkota, R. (2017). "China won't listen; Nepal can act: 20 photos of Araniko Highway after disaster." *Annapurnapost*, http://annapurnapost.com/news-details/80399 (in Nepali).

Shrestha, H. R. (2010). "Road vs. hill environment: The trend of road construction in Nepal, Transport in mountains." *An international Workshop*, Kathmandu, Nepal.

Sidle, R. C., Furuichi, T., and Kono, Y. (2010). "Unprecedented rates of landslide and surface erosion along a newly constructed road in Yunnan, China." *Nat. Hazards*, Vol. 57, No. 2, pp. 313-326, DOI: 10.1007/s11069-010-9614-6.

Sthapit, K. and Tennyson, L. (1991). "Bio-engineering erosion control in Nepal." *Unasylva-No. 164-Watershed Management, An International Journal of the Forestry and Food Industries*, Vol. 42, No. 1991/1, http://www.fao.org/docrep/u1510e/u1510e04.htm.

Stocking, M. (1972). "Relief analysis and soil erosion in Rhodesia using multivariate techniques." *Zeitschrift für Geomorphologie*, Vol. 16, pp. 432-443.

Swets, J. A. (1988). "Measuring the accuracy of diagnostic systems." *Science*, Vol. 240, No. 4857, pp. 1285-1293, DOI: 10.1126/science.3287615.

Tien Bui, D., Ho, T. C., Revhaug, I., Pradhan, B., and Nguyen, D. (2014a). *Landslide susceptibility mapping along the national road 32 of vietnam using GIS-based J48 decision tree classifier and its ensembles*, Springer Berlin Heidelberg, DOI: 10.1007/978-3-642-32618-9_22.

Tien Bui, D., Lofman, O., Revhaug, I., and Dick, O. B. (2011). "Landslide susceptibility analysis in the Hoa Binh province of Vietnam using statistical index and logistic regression." *Nat. Hazards*, Vol. 59, No. 3, pp. 1413-1444, DOI: 10.1007/s11069-011-9844-2.

Tien Bui, D., Pradhan, B., Revhaug, I., and Tran, C. T. (2014b). *A comparative assessment between the application of fuzzy unordered rules induction algorithm and J48 decision tree models in spatial prediction of shallow landslides at Lang Son City, Vietnam*, Springer, DOI: 10.1007/978-3-319-05906-8_6.

Tien Bui, D., Tuan, T.A., Klempe, H., Pradhan, B., and Revhaug, I. (2016). "Spatial prediction models for shallow landslide hazards: A comparative assessment of the efficacy of support vector machines, artificial neural networks, kernel logistic regression, and logistic model tree." *Landslides*, Vol. 13, No. 2, pp. 361-378, DOI: 10.1007/s10346-015-0557-6.

Timilsina, M., Bhandary, N. P., Dahal, R. K., and Yatabe, R. (2014). "Distribution probability of large-scale landslides in central Nepal." *Geomorphology*, Vol. 226, pp. 236-248, DOI: 10.1016/j.geomorph.2014.05.031.

Upreti, B. (2001). "The physiography and geology of Nepal and their bearing on the landslide problem." *Landslide Hazard Mitigation in the Hindu Kush-Himalayas*, pp. 31-49.

USAID Nepal (2015). "Nepal Historical Annual and Monthly Rainfall Distribution." Vol. April 04, No. 2017.

Yang, I. T., Acharya, T. D., and Lee, D. H. (2016). "Landslide susceptibility mapping for 2015 earthquake region of Sindhupalchowk, Nepal using frequency ratio." *Journal of the Korean Society of Surveying, Geodesy, Photogrammetry and Cartography*, Vol. 34, No. 4, pp. 443-451, DOI: 10.7848/ksgpc.2016.34.4.443 .

Yilmaz, I. (2009). "Landslide susceptibility mapping using frequency ratio, logistic regression, artificial neural networks and their comparison: A case study from Kat landslides (Tokat—Turkey)." *Comput. Geosci.*, Vol. 35, No. 6, pp. 1125-1138, DOI: 10.1016/j.cageo.2008.

08.007.

Youssef, A. M., Pradhan, B., Al-Kathery, M., Bathrellos, G. D., and Skilodimou, H. D. (2015). "Assessment of rockfall hazard at Al-Noor Mountain, Makkah city (Saudi Arabia) using spatio-temporal remote sensing data and field investigation." *J. Afr. Earth Sci.*, Vol. 101, pp. 309-321, DOI: 10.1016/j.jafrearsci.2014.09.021.

Zhang, G., Cai, Y., Zheng, Z., Zhen, J., Liu, Y., and Huang, K. (2016). "Integration of the statistical index method and the analytic hierarchy process technique for the assessment of landslide susceptibility in Huizhou, China." *CATENA*, Vol. 142, No. Supplement C, pp. 233-244, DOI: 10.1016/j.catena.2016.03.028.